

# Effect of the Presence of Diblock Copolymer on the Nonlinear Elastic and Viscoelastic Properties of Elastomeric Triblock Copolymers

Alexandra Roos<sup>†</sup> and Costantino Creton\*

UMR 7615, Laboratoire de Physico-Chimie des Polymères et des Milieux Dispersés, ESPCI, 10, Rue Vauquelin, 75231 Paris Cedex 05, France

Received February 15, 2005; Revised Manuscript Received June 28, 2005

**ABSTRACT:** The mechanical properties of blends of triblock and diblock copolymers of polystyrene (PS) and polyisoprene (PI) containing 15 wt % PS have been investigated with tensile tests, relaxation tests, dynamic mechanical tests, and hysteresis tests. The properties of binary triblock/diblock blends have been investigated in parallel with those of the same blends diluted with 60 wt % of a low molecular weight but high- $T_g$  solvent, miscible with the PI component but not with the PS domains. Both binary and ternary blends show a nonlinear elastic behavior at large strains, which can be analyzed with rubber elasticity models, and a pronounced nonlinear viscoelastic behavior at intermediate strains. The analysis of the viscoelastic behavior beyond the linear regime shows that the proportion of PI blocks effectively bridging two PS domains controls the deformation of the blends at large strains, while the small and intermediate strain behavior is controlled by the density of entanglements in the rubbery component and by the relaxation of the PI block of the PS–PI diblock. Both of these nonlinear features depend on the diblock/triblock ratio in the blend and will have direct consequences on more complex properties such as fracture or adhesive debonding.

## 1. Introduction

While thermodynamic and morphological studies of block copolymers abound, investigations of their mechanical properties are much less common. Part of the reason is that block copolymers are often used as the minority component in blends, and their role as emulsifying agent or interfacial reinforcing agents<sup>1</sup> has been mainly emphasized. However, in some applications block copolymers are the majority component and provide the structure of the material. This is the case in particular for the so-called thermoplastic elastomers. These materials are typically based on block copolymers with a glassy block which forms individual domains acting as physical cross-links and an elastomeric block which gives it its rubbery behavior. We investigate in this paper the mechanical properties of a specific type of block copolymer system typically used as a base component for soft pressure-sensitive adhesives.<sup>2</sup> The glassy block is PS and the rubbery block is PI, and all polymers have been synthesized by anionic polymerization.

The PS–PI and PS–PI–PS block copolymers that are used in soft adhesives applications usually have 15–25 wt % of PS and have total molecular weights between 70 and 180 kg/mol. Once they are blended with a small molecule of high  $T_g$  usually called tackifying resin, the volume fraction of PS rarely exceeds 12%. For those compositions and molecular weights, their order–disorder transition temperature is well above room temperature, and the blends are constituted of ordered spheres of PS in a matrix of PI. At room temperature the elastomeric PI matrix is physically cross-linked by the glassy PS domains. Hence, as long as the system is ordered, it can be considered as an elastomer with the

PS domains acting as both physical cross-links and rigid fillers.<sup>3,4</sup> The effect of incorporating a tackifying resin in the PI domains only is to increase the monomer friction coefficient in those domains and to reduce the value of the elastic modulus in the plateau zone.<sup>5</sup>

These materials can be also modeled as a filled elastomer where the PS domains are considered the hard fillers. In that case the classical expression of Guth<sup>6</sup> can be used to predict the value of the plateau modulus as a function of PS content:

$$G_n^0 = \frac{\rho RT}{M_e} (1 + 2.5c + 14.1c^2) \quad (1)$$

where  $G_n^0$  is the plateau modulus,  $\rho$  is the density,  $M_e$  is the molecular weight between entanglements of PI, and  $c$  is the concentration of “fillers”. For adhesive blends containing tackifying resins, the effect of dilution due to the tackifying resin can be expressed by the classical expression for semidilute solutions in a good solvent,<sup>7</sup> i.e.

$$G_n^0(\text{dilute}) = \varphi^{2.25} G_n^0(\text{undilute}) \quad (2)$$

where  $\varphi$  is the polymer volume fraction. Equation 2 assumes that all the tackifying resin, which can be considered as a solvent, is incorporated in the PI domains. For our materials and our resin this is not strictly true. However, only a small fraction of the resin (of the order of 5%) is incorporated in the PS domains.<sup>8</sup> Both eqs 1 and 2 have been recently experimentally verified on adhesive systems. The effect of adding PS–PI diblock chains to PS–PI–PS triblock chains has been investigated in detail by Gibert et al.<sup>9</sup> They concluded that the presence of diblock chains introduced an additional relaxation time corresponding to the relaxation of the free end of the PS–PI alone. On the basis of their results, they proposed a complete molecularly based model to describe the linear viscoelastic

<sup>†</sup> Current address: Essilor International, Lens Materials & Technology, 57, avenue de Condé, Saint-Maur-des-Fossés Cédex 94106, France.

\* To whom correspondence should be addressed.

properties of (PS-PI-PS + PS-PI + resin) blends over the entire range of frequencies. At very low frequencies, they considered the triblock chains as forming a fractal gel with inert PS filler particles. Then they assumed that the relaxation of the diblock chains was analogous to that of the arm of a star or of a tethered chain. Finally, they included the diluting effect of the resin to predict the plateau modulus and a high-frequency relaxation mode to predict the transition zone.

In the previous section we have briefly discussed the linear viscoelastic properties of blends of diblock and triblock copolymers. It is important to keep in mind that while these properties are highly relevant, they only characterize the behavior of the block copolymer below 10% deformation. Yet, it is well-known that the debonding of a polymeric adhesive involves a substantial degree of chain stretching which can only be achieved at deformations of several hundred percent.<sup>10–13</sup>

The deformation of thermoplastic elastomers to large strains (~1000%) raises some specific questions: Are the nanoscopic/macroscale deformations affine? How is the nanostructure affected by the extension? Is the deformation reversible or is there a hysteresis? Is the hysteresis analogous to what is observed for filled chemically cross-linked rubbers (the so-called Mullins effect<sup>14,15</sup>)? What is the effect of adding diblock chains and resin to triblock chains?

Some of these questions have been addressed when thermoplastic elastomers first became commercial. However, nearly all studies consider triblock copolymers alone.

A clear hysteresis upon loading and unloading to large strains was observed by Kaelble et al.<sup>16</sup> on a certain type of commercial PS-polybutadiene (PB)-PS triblock copolymers (Kraton 101). They observed however structures scattering light which led to their interpretation of the hysteresis in terms of cavitation between the PS and PB phases. This observation was not reproduced by Chen and Cohen,<sup>17</sup> who observed a slight Mullins effect and much less hysteresis on research grade PS-PB-PS exhibiting a structure formed of spheres of PS.

Several authors observed the pronounced nonlinear behavior of the stress-strain curve that they obtained for triblock copolymers, and Holden et al.<sup>18</sup> successfully fitted their data for various triblock copolymers with a constitutive equation incorporating both the nonlinear behavior and the filler effect due to the presence of PS spherical domains. They correctly remarked that the peculiar behavior of the thermoplastic elastomers was due to the presence of both fillers and entanglements.

Some authors evoked the possibility of extracting PS end blocks from PS domains under an external stress, implying then that the PS domains do not act as inert fillers only. At intermediate temperatures, the PS domains become softer and the pullout of PS blocks from a PS domain could occur when the PI center blocks become highly extended. Obviously, this pullout must depend on the details of the conformation of the PI chains:<sup>19</sup> a chain effectively forming a bridge between two PS domains will transfer the stress more efficiently than a chain forming a loop (except if the behavior of the latter is modified by the presence of trapped entanglements). Hotta et al.<sup>20</sup> also suggested that the elastomeric network formed by block copolymer systems was transient: above ~30 °C the PS domains would be “breakable cross-links”, by a mechanism of chain pull-

out. Prasman and Thomas studied a (PS-PI-PS + resin) blend constituted of spheres of PS hexagonally packed in a matrix of PI + resin. The blend was stretched to 300% in a simultaneous tensile-SAXS experiment.<sup>21</sup> The authors observed that the nanoscopic lattice was deforming affinely and fully reversibly with the macroscopic deformation. Moreover, they showed that the PS domains kept their spherical shape under extension.

In our investigation we focused specifically on the effect of adding a controlled amount of diblock copolymer to a triblock copolymer. Furthermore, in order to use systems closely resembling those used in adhesive applications, we also tested the same blends with the addition of a constant amount of tackifying resin.

Both copolymers had a PS weight fraction of 15%, and the molecular weight of the diblock was one-half that of the triblock. We prepared four blends of PS-PI-PS and PS-PI to vary the diblock/triblock ratio. The properties of neat copolymer blends and copolymer blends with tackifying resin were investigated in the large strain nonlinear regime by performing tensile tests at different strain rates, relaxation experiments, and hysteresis experiments.

## 2. Theoretical Background

The type of stress-strain curves that are measured for our block copolymer blends in uniaxial extension resembles closely the stress-strain curves measured for cross-linked rubbers. Hence, it seemed logical to use rubber elasticity theory to analyze our data.

The statistical theory of rubberlike elasticity, also called affine theory or neo-Hookean in the solids mechanics community, predicts the nonlinear behavior at large strains of a rubber in uniaxial extension with the following relationship:

$$\sigma_N = G(\lambda - 1/\lambda^2) \quad (3)$$

where  $\sigma_N$  is the nominal stress  $F/A_0$  (with  $F$  the measured tensile force and  $A_0$  the cross section of the undeformed sample),  $\lambda$  is the extension ratio  $l/l_0$  (with  $l$  and  $l_0$  being the length of the deformed sample and undeformed sample, respectively), and  $G$  is the shear modulus. Realizing the shortcomings of this simple model, extensive work has been subsequently carried out to account for the observed nonlinear elastic behavior of cross-linked rubbers. The reader is referred to textbooks<sup>22</sup> and recent reviews<sup>23</sup> for further information.

Among the models that have been proposed, two will be now described in more detail and used to analyze our experimental data: a phenomenological model first proposed by Mooney<sup>24</sup> and further developed by Rivlin<sup>25</sup> which is based on the incompressibility condition and introduces a  $\lambda$ -dependent term in the modulus and a recently proposed molecular model which accounts very well for the entanglements.

In uniaxial extension, Mooney and Rivlin proposed a semiempirical equation, which quantifies the deviation from the neo-Hookean case

$$\sigma_N = 2\left(C_1 + \frac{C_2}{\lambda}\right)\left(\lambda - \frac{1}{\lambda^2}\right) \quad (4)$$

where  $C_1$  and  $C_2$  are two material constants. Note that the reduced stress, defined by

$$\sigma_R = \frac{\sigma_N}{\left(\lambda - \frac{1}{\lambda^2}\right)} \quad (5)$$

depends on the deformation while it did not for the simple affine model.

Much effort has been dedicated to the development of better molecularly based models, which have been discussed in an excellent recent review.<sup>23</sup> Since our block copolymer blends are not strictly speaking rubbers, any quantitative comparison between our data and a molecularly based model should be taken with caution. We feel however that the insight provided by the molecularly based model is essential for the understanding of the mechanical properties of our systems.

A particularly insightful molecular model for the nonlinear elasticity of polymer networks was proposed by Rubinstein and Panyukov:<sup>23</sup> the slip-tube model. In this model the confining potential acting on the network chains depends on the deformation and is modeled by virtual chains attached to the network chains through slip-links, allowed to slip along the contour of the tube but not to pass through each other. The slip-links represent the entanglements points, which are trapped by the cross-linking process.

In the regime of interest, the exact solution for the reduced stress can be well approximated by

$$\sigma_R = G_c + \frac{G_e}{0.74\lambda + 0.61\lambda^{-1/2} - 0.35} \quad (6)$$

where  $G_c$  and  $G_e$  are two physical moduli given by

$$G_c = \left(1 - \frac{2}{\psi}\right)vRT \quad \text{and} \quad G_e = \frac{cRT}{N_e}$$

where  $\psi$  is the network functionality,  $v$  is the total number of elastic strands per unit volume,  $c$  is the monomer concentration, and  $N_e$  is the average number of monomers between entanglements. Therefore,  $G_c$  and  $G_e$  represent respectively the part of the elastic modulus due to the phantom network (fixed) and the part due to the entanglements (slip-links). Note that at small strains, i.e., for  $\lambda \rightarrow 1$ ,  $G_c + G_e$  is equivalent to the shear modulus  $G$ , and for very large strains the stiffness of the material only depends on  $G_c$ , i.e., on the density of cross-links.

### 3. Experimental Section

**3.1. Materials.** The block copolymers used in this study were synthesized by Dexco (Dow Chemicals and ExxonMobil Chemical joint venture). In our study we focused on four PS-PI-PS + PS-PI blends. The main varying parameter is the diblock weight fraction (from no diblock to 54 wt %). The molecular characteristics of these four model blends are given in Table 1. Note that the PS content is kept constant as well as the molecular weights, the diblock chains being roughly half as long as the triblock chains. All indices of polydispersity are inferior to 1.1.

Since for adhesive applications a "tackifying" resin must be used,<sup>26</sup> we also investigated the same blends with a resin.

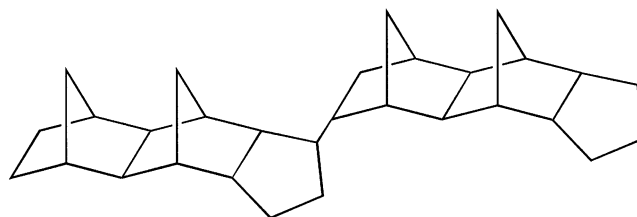


**Figure 1.** Molecular structure of the tackifying resin used in our study.

Various tackifying resins can be used in adhesives, and the choice depends on the polymer that needs to be "tackified" and the target adhesive application. The most popular resins for polyisoprene are from the family often described as hydrocarbon resins (HCR) made from the polymerization of petroleum-derived feedstocks.

We have used a hydrogenated HCR derived from cyclopentadiene produced by ExxonMobil Chemical, known by the trade name Escorez 5380. This type of resin is essentially a rigid molecule containing cyclic C5 and C9 groups as schematically shown in Figure 1. Tackifying resins must be miscible with the rubbery component of the base adhesive polymer but immiscible with the glassy domains. They have the dual function of diluting the entanglement network and increasing the glass transition temperature to give the tacky behavior.<sup>4</sup> Narrow molecular weight distributions are desirable to improve the compatibilities. Polydispersities of the resin are typically about 2. The glass transition temperature of the resin we used (Escorez 5380) was 40 °C.

Two types of samples were prepared: pure block copolymer blends as described in Table 1 and adhesive formulations, containing each 40 wt % of base polymer and 60 wt % of Escorez resin. The block copolymer blends films were all prepared from 14.75 wt % solutions in toluene and subsequently cast in molds adapted to the experiment to be performed and slowly dried.

**3.2. Rheology in the Linear Regime.** The linear viscoelastic properties of the block copolymer systems were obtained from small strain rheological measurements in oscillatory shear. We performed these tests on a rheometer RDA II from Rheometrics in the parallel plates geometry. The samples were prepared from 14.75 wt % solutions in toluene, cast in aluminum pans. They were dried 10 days at room temperature and 48 h at 45 °C under vacuum. Although it is possible that with such a drying procedure a small amount of toluene (<0.1%) remains in the PS phase, the results we obtained are quantitatively consistent with those obtained by Gibert et al. with samples prepared from the melt.<sup>9</sup>

The pellet (~2 mm thick) was placed on the lower plate, and the upper plate was brought into contact with the sample. A light pressure was applied for 10–15 min in order to ensure a good adhesion between the plates and the sample. Then a strain sweep was applied to the sample at a given temperature and a given frequency (typically the highest ~80 Hz) in order to explore the domain of strains where the response of the sample is in the linear regime.

All tests were performed at 22 °C. The data obtained were the storage modulus  $G'$ , the loss modulus  $G''$ , and consequently the loss tangent  $\tan(\delta) = G''/G'$  as a function of the frequency  $\omega/2\pi$ .

**3.3. Tensile Tests.** We performed our tensile tests on a commercial tensile testing machine (JFC TC3) fitted with a 50 N load cell and able to measure displacements up to 400 mm. Samples were cast from the toluene solutions into Teflon molds, for the (sticky) resin blends, or in aluminum pans for

**Table 1. Molecular Characteristics of the Four Model Blends of This Study**

	wt % PS-PI	$M_w(\text{PS-PI-PS})$ , kg/mol	wt % PS in PS-PI-PS	$M_w(\text{PS-PI})$ , kg/mol	wt % PS in PS-PI
Vector 4100 D	0	154	15.1		
Vector 4113	19	154	15.1	72	15
Vector 4114	42	156	15.1	72	15
DPX 565	54	176	16.1	72	16

the pure block copolymers. The samples were dried 10 days at room temperature followed by 48 h at 45 °C under vacuum. The samples tested were rectangular in shape with the following dimensions: 300  $\mu\text{m}$  thick, 4 mm wide, and 15 mm high (length between the clamps). We verified with a video camera that the deformation was macroscopically homogeneous even at large deformations. The samples containing resin were very soft and very adhesive, and they were removed from their Teflon mold by freezing them in liquid nitrogen. They were then placed between two sheets of release paper. The films were cut with scissors at the chosen dimensions and placed in the upper clamp after being frozen in liquid nitrogen. Indeed, the upper clamp being a simple clip, the sample had to be rigid enough to be fixed. The sample was then left to equilibrate for 2–5 min at RT, and the lower clamp was tightened on the film. The tensile tests were then performed at three constant crosshead velocities: 5, 50, and 500 mm  $\text{min}^{-1}$  (corresponding to initial strain rates of  $5.6 \times 10^{-3}$ –0.56 Hz) and at room temperature. They were repeated twice, except for the lowest velocity of 5 mm  $\text{min}^{-1}$ .

It is important to note that tensile tests performed in the large strain regime at constant crosshead velocity do not deform the sample at a constant strain rate. From a materials testing point of view, a proper configuration would have been an exponentially increasing crosshead velocity to compensate for the thinning of the sample cross section as it is being elongated. This was not possible with our setup, but since our materials are not very viscoelastic and display a behavior which is chiefly dependent on strain and not strain rate, we feel that a simple tensile test provided already most of the information. We extracted from our force–displacement curve the nominal ( $\sigma_N$ ) stress as a function of the extension ratio  $\lambda$ . In contrast to many studies on rubber, we use throughout this paper the nominal stress rather than the true stress. This choice was made because the strain softening at intermediate strains is much more apparent when represented in nominal stress terms.

**3.4. Relaxation Tests and Hysteresis Tests.** We performed relaxation tests in both shear and elongational geometries. The shear geometry was used to test the relaxation of SBC-based systems in the linear regime and the elongational geometry to test them in the nonlinear range. The way the samples were prepared is explained in the two previous subsections for each geometry.

In shear, tests of linearity were performed at  $\omega = 500$  rad  $\text{s}^{-1}$  (i.e., 80 Hz) in order to determine the appropriate deformation for the relaxation tests to stay in the linear range (typically from 1 to 5% for our blends). Then this given deformation was applied to the sample<sup>33</sup> in typically 0.06 s, and we measured the relaxation modulus  $G(t)$  as a function of time for  $10^3$ – $10^4$  s. These tests were performed at 25 °C on resin blends only.

In elongation, the relaxation tests were performed at a deformation of 500%. It took 9 s for the crosshead to go to this elongation ( $V_t = 500$  mm  $\text{min}^{-1}$ , i.e., 0.56 Hz). Tests were performed at room temperature, and the relaxation of the stress was measured as a function of time for 1000 s. We tested both pure polymer blends and polymer blends with resin.

Finally, we performed tests based on the classical design used to detect the Mullins effect in rubber + filler materials in order to estimate the dissipative losses in the tensile geometry. The Mullins effect was first observed by Holt:<sup>27</sup> a rubber material filled with carbon black was stretched to a given deformation, and then the stress was released to zero and the sample was stretched again to a higher deformation. The measured stress appeared to be lower up to the first deformation before joining the original tensile curve. Mullins,<sup>14</sup> and later Bueche,<sup>15</sup> attributed this loss in the reinforcement to the progressive breakage of carbon black aggregates and to the breakage of rubber–particles bonds.<sup>14,15</sup>

Therefore, we performed the following tests: The sample was stretched until 100% deformation at  $V_t = 50$  mm  $\text{min}^{-1}$  and went back to zero force at the same velocity. Then, the same sample was stretched successively to 200, 300, 400, and 500% deformation (relative to the same  $L_0$ ), always at the same

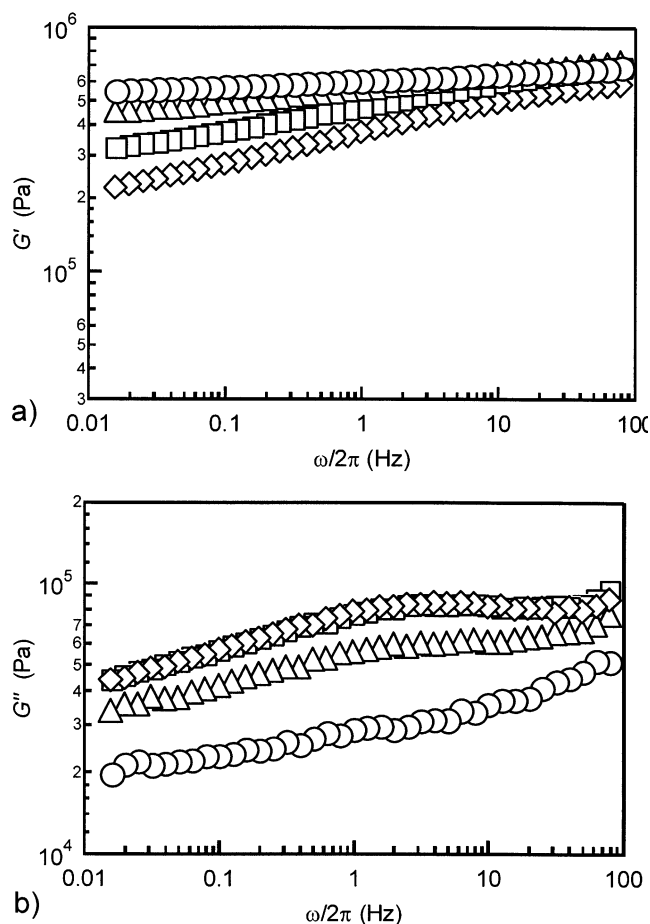


**Figure 2.** (a) Elastic modulus  $G'$  and (b) loss modulus  $G''$  as a function of frequency for various PS–PI contents, at  $T = 22$  °C, for blends without resin:  $\circ$ , 0 wt % PS–PI;  $\triangle$ , 19 wt % PS–PI;  $\square$ , 42 wt % PS–PI;  $\diamond$ , 54 wt % PS–PI.

crosshead velocity for both directions of displacement of the crosshead. The force  $F$  and displacement  $L$  data were recorded, and the nominal stress  $\sigma_N$  and strain  $\epsilon$  were calculated using the initial dimensions of the sample. These tests were performed on both pure polymer and resin blends, at room temperature.

## 4. Results

**4.1. Linear Viscoelastic Properties.** Since a comprehensive study on the effect of the triblock/diblock ratio on the linear viscoelastic properties of block copolymer blends has been recently reported,<sup>9</sup> we only characterized the linear viscoelastic properties of both neat block copolymers and adhesive blends at room temperature and down to frequencies of about 0.01 rad/s.

These results are shown in Figure 2 for the neat block copolymer blends and in Figure 3 for the tackified blends. The reduction in the plateau modulus is evident by comparing Figures 2a and 3a. However, the effect of adding a diblock copolymer to the triblock is very similar for both series of blends. In both cases, the differences appear at low frequency, a regime where the free isoprene end of the diblock chain is able to relax. This relaxation process is analogous to the relaxation of an arm of a starlike polymer<sup>28</sup> and causes  $G'$  to drop to a lower plateau modulus, the level of which is only controlled by the density of triblock chains actually bridging two PS domains.<sup>9</sup> Another notable difference

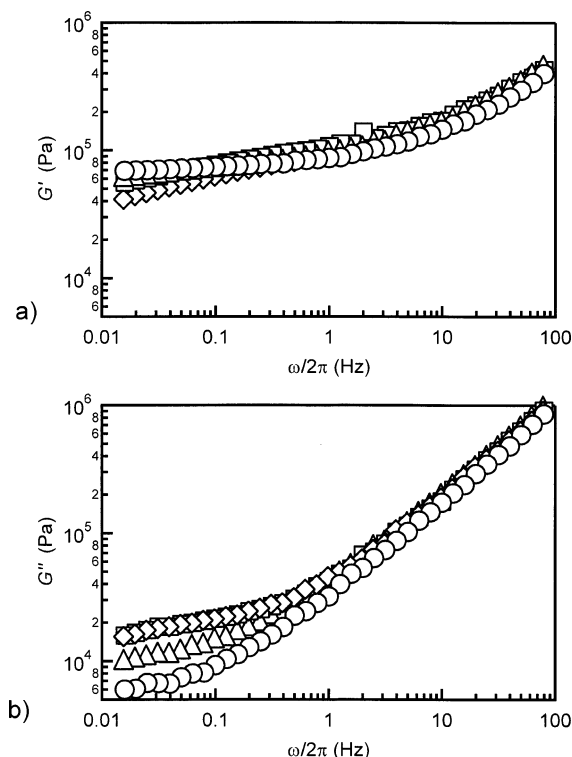


**Figure 3.** (a) Elastic modulus  $G'$  and (b) loss modulus  $G''$  as a function of frequency for various PS-PI contents, at  $T = 22$  °C, for blends with 60 wt % resin:  $\circ$ , 0 wt % PS-PI;  $\triangle$ , 19 wt % PS-PI;  $\square$ , 42 wt % PS-PI;  $\diamond$ , 54 wt % PS-PI.

is the characteristic dissipative character found for adhesive blends at high frequency which is partially responsible for the tacky behavior of the adhesive blends.

**4.2. Nonlinear Elasticity.** The typical shape of a nominal stress ( $\sigma_N$ ) vs extension ratio ( $\lambda$ ) tensile curves for blends without resin is shown in Figure 4. Although the curves of Figure 4 are individual curves and not averages, the reproducibility of the curves is quite good, and the parameters of the fits are represented with error bars in Figures 8 and 10. Further studies on the same materials performed in the same group have shown that the results are not very sensitive to the preparation conditions (i.e., drying conditions, grips). One could furthermore argue that the results should be dependent on the solvent used to cast the films. To check that hypothesis, we have also performed tensile tests on films prepared without any solvent (by blending above the order-disorder transition). Tensile stress-strain curves are, within experimental error, identical to those obtained with films cast from toluene.

The tensile behavior is clearly nonlinear for strains higher than 50%. It does not depend much on the crosshead velocity  $V_t$  over the 2 decades of velocities investigated (Figure 4a). On the other hand, at a given  $V_t$  the effect of diblock content is considerable (Figure 4b): Increasing the PS-PI content leads to lower stresses for all extensions because of a marked softening at intermediate elongations ( $\lambda = 2-6$ ) and a less pronounced hardening at the highest elongations. Moreover, the hardening occurs at higher values of  $\lambda$  for high PS-PI contents. We will not discuss here the values of elongation at break because the samples first began to slip between the clamps before breaking: the curves are thus cut just before the beginning of the slippage process (evidence of slippage at high strain was found by an

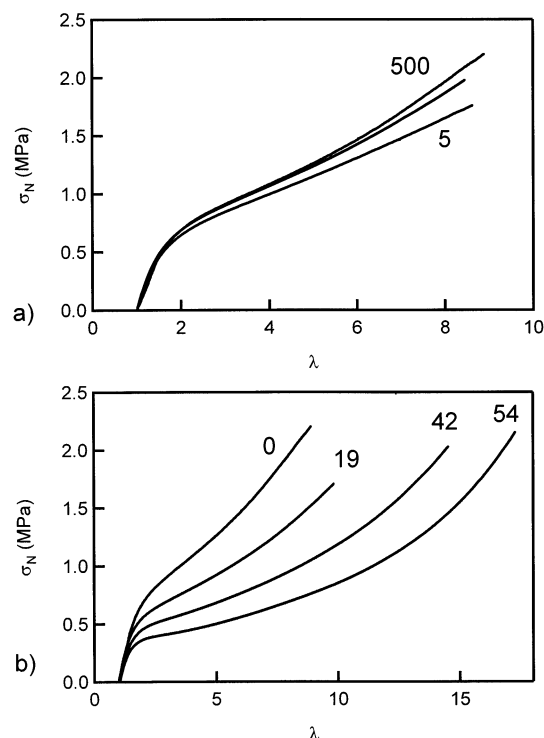


**Figure 4.** Nominal stress as a function of strain for blends without resin: (a) tensile tests for the 0 wt % PS-PI blend at  $V_t = 5, 50$ , and  $500 \text{ mm min}^{-1}$  and (b) tensile tests at  $V_t = 500 \text{ mm min}^{-1}$  for blends with 0, 19, 42, and 54 wt % PS-PI.

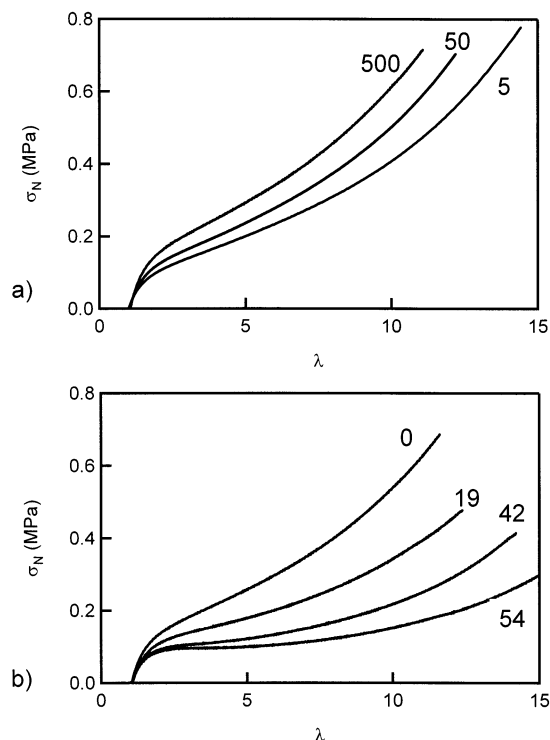


**Figure 5.** Nominal stress as a function of strain for blends with 60 wt % resin. (a) Tensile tests for the 0 wt % PS-PI blend at  $V_t = 5, 50$ , and  $500 \text{ mm min}^{-1}$ . (b) Tensile tests at  $V_t = 500 \text{ mm min}^{-1}$  for blends with 0, 19, 42, and 54 wt % PS-PI.

experiment performed with an optical extensometer). When 60 wt % resin is added, the level of tensile stress drops as shown in Figure 5, but the shapes of the tensile curves stay the same: linear deformation followed by a softening ( $\lambda = 2-8$ ) and a hardening.

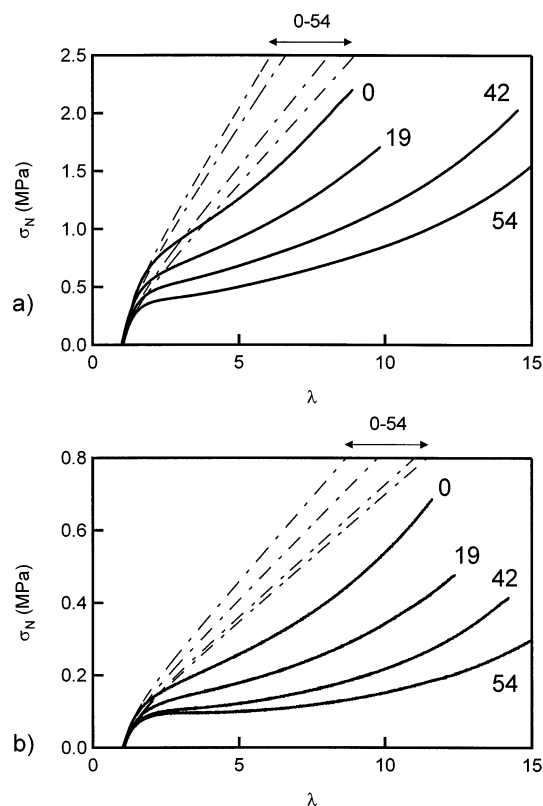


**Figure 6.** Nominal stress as a function of strain for blends containing 0, 19, 42, and 54 wt % PS-PI at  $V_t = 500 \text{ mm min}^{-1}$  (solid lines) and theoretical rubberlike elasticity curves for equivalent elastic moduli (dashed lines): (a) blends without resin and (b) blends with 60 wt % resin.

The adhesive blends are slightly more strain rate dependent than the blends without resin (Figure 5a): Increasing the crosshead velocity  $V_t$  leads to higher stresses. However, the influence of the PS-PI content is the same, with and without resin: the more diblock, the more pronounced is the softening and the more delayed is the hardening at high extension as shown in Figure 5b.

## 5. Analysis

Theoretical rubberlike curves based on eq 3 were plotted in Figure 6 by using the corresponding values of  $G$  measured on our tensile curves (using the relationship for incompressible materials  $E = 3G$ ). While the experimental and predicted curves are identical until  $\lambda = 2$  (same  $E$ ), they diverge at higher strains: the slope of the experimental curve decreases (softening) until it reaches an inflection point and increases again (hardening). Moreover, the more PS-PI in the blend, the more important is the deviation from rubberlike elasticity. Not only the shape of the tensile curves is not well predicted but also the effect of the PS-PI content is underestimated.

The reduced stress is defined as  $\sigma_R = \sigma_N/(\lambda - 1/\lambda^2)$ . Since the prediction of the statistical theory does not fit the data above 20% deformation even for standard cross-linked rubbers, it is usual for larger deformations to fit the experimental data with eq 4, the so-called Mooney-Rivlin equation.

For this purpose the reduced stress  $\sigma_R$  was plotted as a function of  $1/\lambda$  in Figure 7 for both pure copolymers and resin blends. This representation of the data emphasizes more directly the differences with the neo-

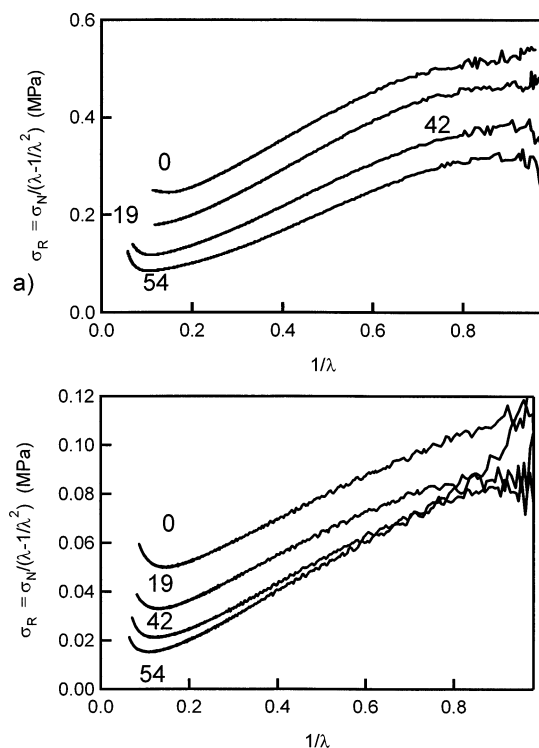


**Figure 7.** Reduced stress as a function of  $1/\lambda$  for blends containing 0, 19, 42, and 54 wt % PS-PI at  $V_t = 500 \text{ mm min}^{-1}$ : (a) blends without resin and (b) blends with 60 wt % resin.

Hookean behavior. Indeed, if one reads Figure 7 from right to left (decreasing  $1/\lambda$ , increasing  $\lambda$ ), one can see that, instead of being constant,  $\sigma_R$  decreases until it reaches a minimum at about  $1/\lambda = 0.1$  and increases again, illustrating the softening followed by the hardening.  $\sigma_R$  does not increase linearly with  $1/\lambda$  over the entire deformation range. However, a linear range can be seen between 200 and 500% deformation, and we performed fits of the experimental data within this range.

A first important result shown in Figure 8 is that for blends with and without resin,  $C_2$  is much larger than  $C_1$ . Furthermore, while  $C_2$  varies little with PS-PI content (a 20% decrease for the pure blends and a 20% increase for the blends with resin),  $C_1$  decreases by more than 80% when going from pure triblock to 54% diblock, regardless of the presence or absence of resin.

Many studies have tried to interpret  $C_1$  and  $C_2$  in molecular terms:  $C_1$  would be associated with both trapped entanglements and cross-links whereas  $C_2$  would be associated only with nonpermanent entanglements.<sup>29</sup> This interpretation was also proposed by Holden et al.<sup>18</sup> to explain the abnormally high modulus that they obtained by fitting the tensile stress-strain curves measured for their SBS triblock copolymers, with a Mooney-Rivlin constitutive equation. Essentially this means that the entanglements play a dominant role in the elasticity of the materials at low strains while the cross-links become important for high  $\lambda$ . What is new, however, is the dramatic effect of the presence of diblock on the value of  $C_1$ . The diblock addition appears to reduce the number of effective cross-links relative to number of entanglements. This is consistent with the fact that, since the diblock used in this study has a molecular weight which is half that of the triblock and has the same PS content, increasing the PS-PI content is equivalent to replacing one triblock with two diblocks.

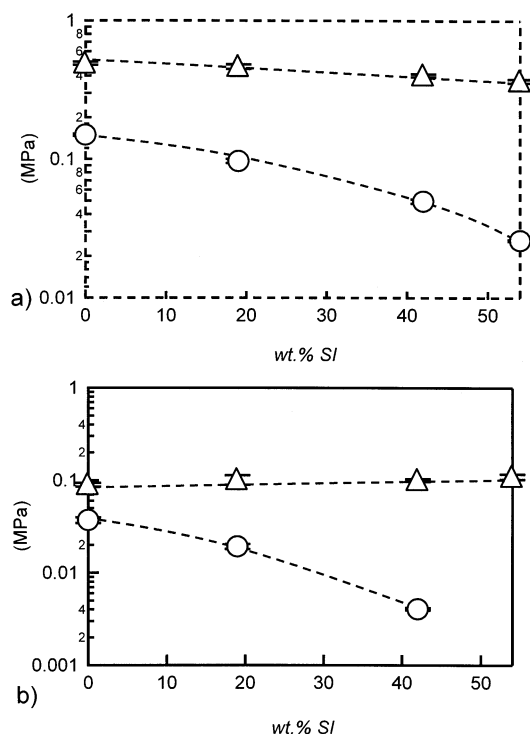


**Figure 8.** Mooney–Rivlin coefficients as a function of PS–PI content at  $V_t = 500 \text{ mm min}^{-1}$ : (○)  $2C_1$ ; (△)  $2C_2$ ; (a) blends without resin; (b) blends with 60% resin. The dashed lines are a guide to the eye.

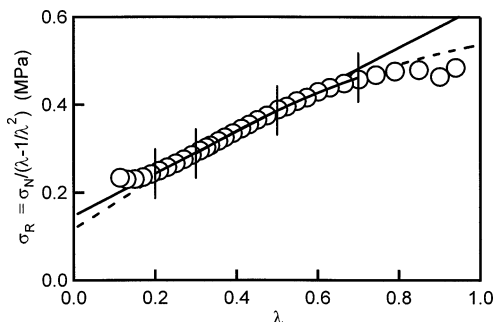


**Figure 9.** Best intervals for the different fits of tensile curves: (○) experimental curve, (—) Mooney–Rivlin fit, (---) slip-tube model fit.

This loss of connectivity causes a loss of bridging elastic strands in the material.

Although the details of the molecular structure are different, it is interesting to fit the data with a recent molecular analysis of the elasticity of polymer networks proposed by Rubinstein and Panyukov: the slip-tube model<sup>23</sup> which has been described in more detail earlier.

The fits of our data to the slip-tube model were only good for the intermediate strain regime ranging from 125% to 333%. Note that this interval is different than the one preferred for Mooney–Rivlin fits because of the particular shapes of the reduced stress curves. As Figure 9 shows, the slip-tube model fits better the bending of the curve at low-intermediate strains while the Mooney–Rivlin equation fits better the linear part at intermediate–high strains. Neither model can fit the hardening at large strains since strain hardening is not built in the model.

Moreover, whereas the linear fits for Mooney–Rivlin equation were possible for all experimental conditions, we could not fit the 60 wt % resin–42 and 54 wt %

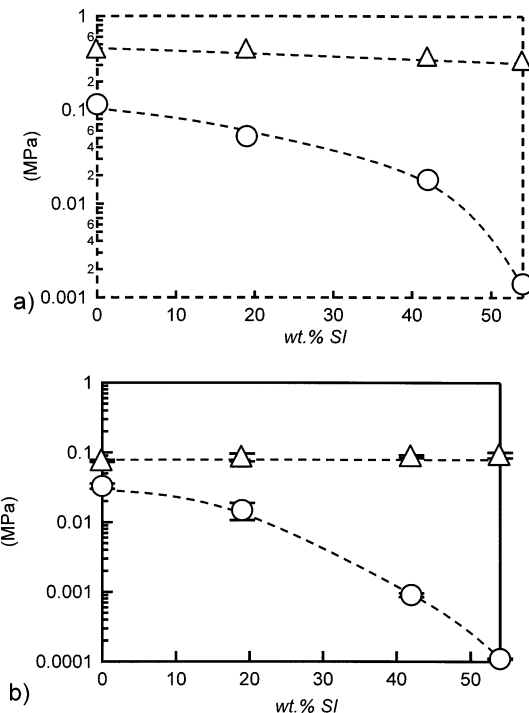


**Figure 10.** Slip-tube model coefficients (○,  $G_c$ ; △,  $G_e$ ) as a function of PS–PI content for (a) blends without resin and (b) blends with 60 wt % resin. The dashed lines are a guide to the eye.

blends at the lowest crosshead velocities  $V_t = 5$  and  $50 \text{ mm min}^{-1}$  with the slip-tube model: In these cases the fitting interval was too short, and we sometimes obtained unphysical negative values for  $G_c$ ! This suggests that adding resin molecules and/or diblock chains leads to materials, which cannot be fitted successfully by models based on rubber elasticity like the slip-tube model.

Figure 10 confirms that for all blends the entanglement modulus  $G_e$  is significantly larger than the crosslink modulus  $G_c$ . For neat block copolymer blends,  $G_c$  and  $G_e$  decrease with an increase in the PS–PI content, and for adhesive blends,  $G_c$  decreases and  $G_e$  remains constant. From the molecular standpoint this result suggests that PS–PI–PS + PS–PI and PS–PI–PS + PS–PI + resin blends can indeed be described as weakly cross-linked but highly entangled rubbers, the major part of the elastic modulus  $G_c + G_e$  being due to the entanglements of the polyisoprene matrix. The decrease of  $G_c$  is consistent with the fact that increasing the PS–PI content is equivalent to replacing one triblock with two diblocks.

Although qualitatively correct, this interpretation can also be quantitatively checked. Using a combination of eqs 1, 2, and 6, the nominal stress in uniaxial extension can be written as

$$\sigma_N = (1 + 2.5\phi_{PS} + 14.1\phi_{PS}^2) \left( \lambda - \frac{1}{\lambda^2} \right) \left( G_c + \frac{G_e}{0.74\lambda + 0.61\lambda^{-1/2} - 0.35} \right) \quad (7)$$

All parameters in this expression are known. For neat block copolymer blends,  $\phi_{PS} = 0.144$ ,  $G_e$  is taken as the plateau modulus at  $25^\circ\text{C}$  of PI,1,4 and is equal to 0.35 MPa.<sup>30</sup> This assumption implies that the free chain ends of the diblocks all contribute to the entanglement network. As pointed out by Daoulas et al., these

**Table 2.** Detailed Comparisons of the Experimentally Fitted Values of  $G_c$  and  $G_e$  and of the Calculated Values

fitted/calculated	$G_e$ (kPa)			
	0 wt % PS-PI	19 wt % PS-PI	42 wt % PS-PI	54 wt % PS-PI
0 wt % resin	440 ± 20/350	440 ± 20/350	370 ± 20/350	330 ± 20/350
60 wt % resin	81 ± 3/35	82 ± 2/35	88 ± 2/35	91 ± 2/35
fitted/calculated	$G_c$ (kPa)			
	0 wt % PS-PI	19 wt % PS-PI	42 wt % PS-PI	54 wt % PS-PI
0 wt % resin	115/11.6	52/9.4	18/6.7	1.4/4.7
60 wt % resin	26 ± 2/4.7	12 ± 2/3.8	0.9/2.7	0.1/1.9

dangling ends can be modeled as arm stars, and their relaxation time is of the order of 150 s at room temperature.<sup>8</sup> Hence, in particular for the tensile tests performed at 500 mm min<sup>-1</sup> which only last 20–30 s, we can reasonably assume that all entanglements contribute to the modulus and that  $G_e$  has a fixed value for all the undiluted blends. For the blends with resin, the problem is more complicated. The relaxation time of the arm star will be modified in two ways relative to the undiluted blends: it will be increased by the shift in glass transition temperature brought by the high- $T_g$  resin which will modify the friction coefficient and decreased by the change in the average molecular weight between entanglements (which increases as  $\phi^{-5/4}$ ). It should be noted that although the solubility of the resin in PS is not zero (on the basis of the different  $\chi$  parameters of the system, Daoulas et al.<sup>8</sup> report here a volume fraction of resin of 5% in the PS domains from self-consistent mean-field simulations), it is sufficiently small to be neglected in the interpretation of our results.

$G_c$ , on the other hand, is given by the density of network strands, i.e., the density of PS-PI-PS triblock chains bridging two PS domains. The functionality of the network is certainly large here, and the phantom network correction can be neglected. The self-consistent mean-field simulations of Daoulas et al.<sup>8</sup> have shown that for all blends ~80% of the triblock chains are bridging irrespective of the amount of diblock or resin present in the blend. We can then assume that  $G_c$  is given by

$$G_c = \nu kT = 0.8 \frac{\rho_{PI} RT}{M_{PI(SIS)}} \phi_{PI} \phi_{tri} \quad (8)$$

where  $\rho_{PI}$  is the density of PI,  $M_{PI(PS-PI-PS)}$  is the molecular weight of the PI block in the triblock,  $\phi_{PI}$  is the volume fraction of PI in the blend, and  $\phi_{tri}$  is the volume fraction of triblock in the polymer blend.

For blends diluted with the resin, both  $G_c$  and  $G_e$  are reduced. The entanglements are reduced according to eq 2 so that

$$G_e(\text{dilute}) = \varphi^{2.25} G_e(\text{undilute}) \quad (9)$$

Cross-link points are simply diluted by the volume fraction so that

$$G_c(\text{dilute}) = \varphi G_c(\text{undilute}) \quad (10)$$

Detailed comparisons of the experimentally fitted values of  $G_c$  and  $G_e$  and of the calculated values are given in Table 2.

An alternative way to compare the data is to plot the simulated curves alongside the experimentally measured ones. Figure 11a,b shows this comparison for the pure blends and the diluted ones.

The quantitative comparisons between theory and experiment in Figure 11 highlight two aspects:

(i)  $G_e$  in the pure polymer blends is well predicted quantitatively by the value of  $G_N^0$  in pure polyisoprene. However, for the diluted blends, the tensile tests give systematically higher values of  $G_e$  than what a simple dilution of the entanglements in a good solvent would give. This discrepancy may be due to viscoelastic effects although we do not see a very large effect of strain rate as shown in Figure 5a. It is possible that the entanglement structure is affected by the casting method (casting solvent in particular) and does not hence obey a simple dilution law. However, at this stage we do not have clear evidence that this is an important effect, and experiments performed on blends prepared from the melt show nearly identical stress-strain curves.<sup>31</sup>

(ii) Both in the undiluted and in the diluted blends, the quantitative effect of replacing a triblock copolymer with two diblocks greatly exceeds the theoretical predictions. This point is remarkable since such a large effect on the nonlinear elastic properties has important consequences on more complex properties which depend on the large strain behavior of the material such as fracture and adhesion.<sup>31</sup>

Finally, it is interesting to discuss the possibility of pullout of the PS chains from the PS domains. The two

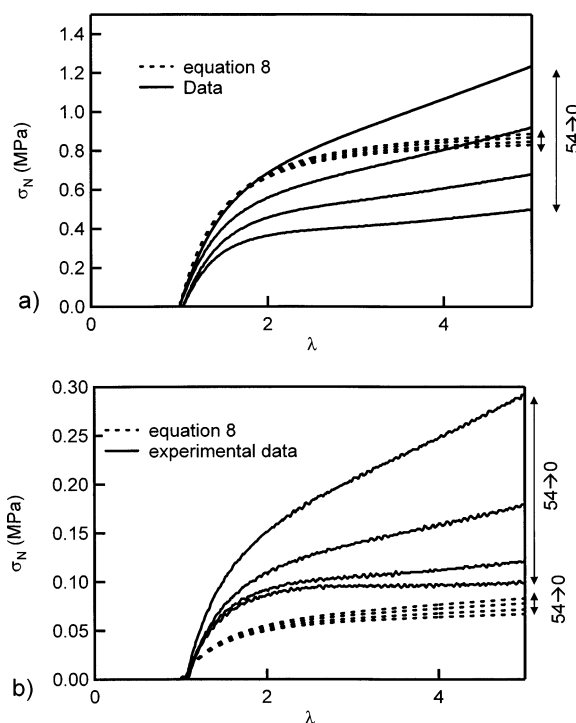


**Figure 11.** Nominal stress as a function of strain (full line) for blends containing 0, 19, 42, and 54 wt % PS-PI ( $V_t = 500$  mm min<sup>-1</sup>) and theoretical predictions from eq 8: (a) blends without resin and (b) blends with 60% resin.

**Table 3. Predicted Pullout Stress Based on the Measured Value of  $G_c$  (Table 2)**

	0 wt % PS-PI	19 wt % PS-PI	42 wt % PS-PI	54 wt % PS-PI
0 wt % resin	550	250	86	6.7
60 wt % resin	125	57	4.3	0.5

parameters which we know are the volume density of bridging chains and the average distance between domains  $d$  which is independent of the composition of the blends<sup>8</sup> and is  $\sim 30$  nm for our blends. If we suppose that the physical cross-linking is homogeneous through the material, we can write that the areal density  $\Sigma$  of chains across a given plane are given by

$$\Sigma = \frac{G_c d}{kT} \quad (11)$$

If we use the measured value of  $G_c$  obtained from the fits of the tensile data with the slip-tube model, we obtain a range of values varying from  $7 \times 10^{14}$  for the adhesive blend with 54% diblock to  $8.4 \times 10^{17}$  chains/m<sup>2</sup> for the pure triblock PS-PI-PS. The minimum static force to pullout a PS chain from a glassy PS matrix at room temperature was estimated from independent studies of chain pullout<sup>32</sup> at  $\sim 6$  pN/monomer. For our PS blocks this corresponds to a minimum pullout force of 0.66 nN/PS chain. Table 3 shows this pullout stress for the eight materials of this study. This stress should be compared with the nominal tensile stress applied to the material “since we assumed that the material was isotropic for the calculation of the areal density of chains. Such a comparison immediately shows that chain pullout from the PS domains is very unlikely at room temperature, except for the 54% diblock and 60% resin material. If instead of using the fitted values of  $G_c$  we use the predicted values from the self-consistent-field simulation, neglecting therefore trapped entanglements, the probability of pullout increases somewhat but remains very unlikely for all materials except the 54% diblock with resin.

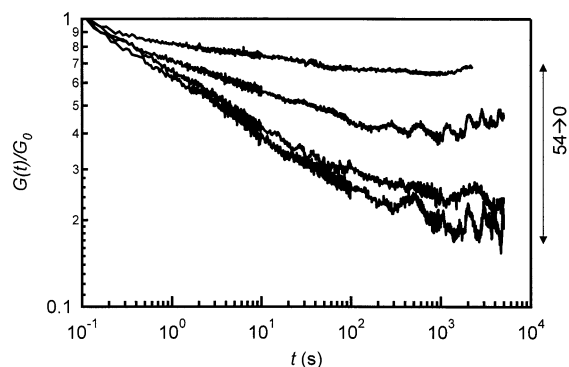
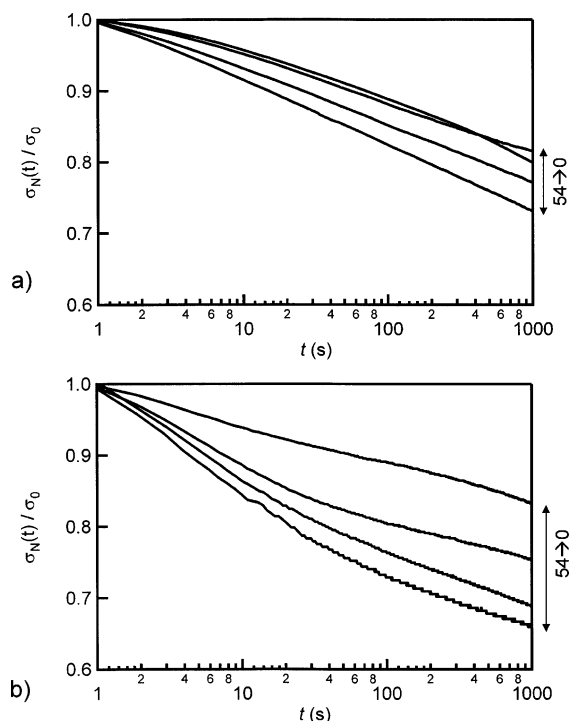
## 6. Complementary Tests

**6.1. Relaxation Tests.** The relaxation behavior of pure blends and resin blends were investigated in both shear and elongation. The shear geometry was used in the linear regime and the elongational geometry in the nonlinear range.

The relaxation moduli normalized by the moduli at the beginning of the relaxation ( $G_0$ ) are presented in Figure 12 for the four model resin blends at room temperature. The values of  $G_0$  are given in Table 4 and follow the values of the elastic modulus  $G'$  at  $\sim 17$  Hz (which corresponds to the frequency applied to the sample during the deformation step):  $G_0$  is independent of the PS-PI content (but always lower than  $G'$ ).

The material relaxes more when there is more diblock in the blend: namely from 30 to 85% of the stress after an imposed deformation of  $\gamma = 2\%$ . In all cases the relaxation seems to be over after 1000 s.

In the elongational geometry, the samples were rapidly (in 9 s) stretched to a deformation of 500% before recording the relaxation of the stress. Figure 13 shows the relaxation of the stress normalized by the level of stress at the beginning of the relaxation for both pure polymer blends and resin blends at room temperature. Unlike in the linear regime, the levels of stress at the

**Figure 12.** Relaxation modulus in shear for the blends with 60 wt % resin at room temperature after a deformation  $\epsilon = 2\%$ .**Figure 13.** Relaxation of the stress in elongation at room temperature after a deformation  $\epsilon = 500\%$  for (a) blends without resin and (b) blends with 60 wt % resin.**Table 4. Moduli at the Beginning of the Relaxation ( $G_0$ ) Compared to Elastic Moduli Measured in Linear Viscoelasticity ( $G'$ ) at 17 Hz**

	0 wt % PS-PI	19 wt % PS-PI	42 wt % PS-PI	54 wt % PS-PI
$G_0/G'$ (kPa)	105/171	87.1/200	91.3/210	89.2/197

**Table 5. Levels of Stress  $\sigma_0$  at the Beginning of the Relaxation**

$\sigma_0$ (MPa)	0 wt % PS-PI	19 wt % PS-PI	42 wt % PS-PI	54 wt % PS-PI
0 wt % resin	1.257	0.880	0.666	0.490
60 wt % resin	0.283	0.208	0.143	0.085

beginning of the relaxation decrease with an increasing diblock and resin contents. These values of  $\sigma_0$  are given in Table 5. This is however not surprising since in the tensile geometry the stretch to 500% deformation takes several seconds, and some relaxation can take place already during this loading stage. Similarly to what is observed in the linear regime, the more diblock in the blend the more rapid and pronounced is the relaxation.

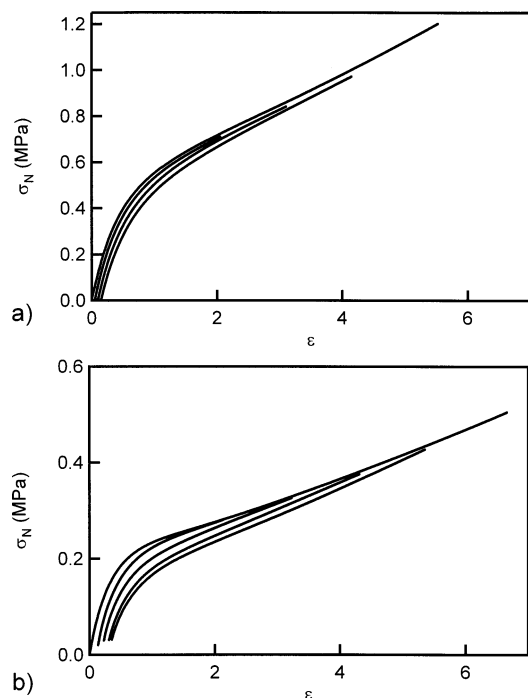


**Figure 14.** Consecutive tensile tests for the blends without resin: (a) 0 wt % PS-PI; (b) 54 wt % PS-PI. The leftmost curve is the first test, and subsequent tests start at increasingly high levels of residual deformation.

However, the similarity ends here. After 1000 s, the material only relaxes 18–27% of the initial applied stress for pure polymer blends and 18–34% of the stress for adhesive formulations. In addition, in all cases the relaxation processes is not over after 1000 s.

Interestingly, the presence of resin does not affect much the total relaxation over a 1000 s time even though the blends with resin and diblock relax a little faster. However, the shape of the stress vs time curve is not the same: the decrease of the stress is faster when there is 60 wt % resin, especially during the first 50 s.

These two experiments show that there is a remarkable difference in the kinetics of relaxation at small and large strains. Indeed, small-strain relaxation is in the linear viscoelastic regime whereas the relaxation tests performed in the tensile geometry involve the nonlinear viscoelastic properties of the material: When the sample is stretched to large strains, the relaxation of the polymeric chains occurs in a strongly oriented network at a rate which depends probably mainly on the relaxation of the triblock chains bridging between PS domains. On the other hand, at small strains most of the stress, and then of the relaxation, occurs between entanglements, which are present in much larger densities ( $G_e \gg G_c$ ) and relax faster than the central PI blocks of the triblocks.

**6.2. Hysteresis and Residual Strain.** As a final characterization of the large strain behavior, we performed consecutive tensile tests following a methodology used for detecting the Mullins effect in rubber + filler materials,<sup>14</sup> i.e., successive tensile tests on the same sample. Large differences between the first tensile test and the following tensile tests are indications of very slow relaxation processes in the material and of the destruction of a structure during the tensile test.

Figure 14 and Figure 15 show the results obtained for blends without resin and with 60 wt % resin at room

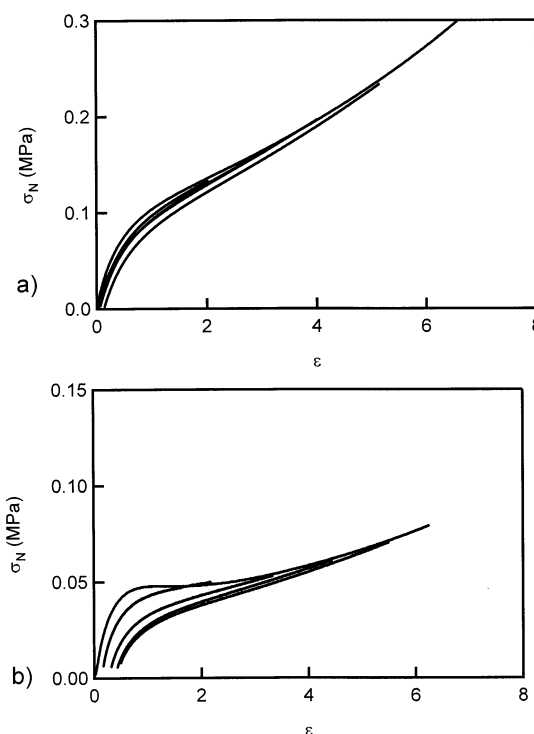


**Figure 15.** Consecutive tensile tests for the blends with 60 wt % resin: (a) 0 wt % PS-PI; (b) 54 wt % PS-PI. The leftmost curve is the first test, and subsequent tests start at increasingly high levels of residual deformation.

temperature. On each graph the successive tensile tests performed on one given sample, and a simple tensile test performed on another sample as a reference, are plotted.

For the pure triblock material (Figure 14a) all the curves can be nearly superimposed: the residual deformation is negligible. However, the more diblock in the blend, the more different becomes the stress-strain curve when successive tractions are performed as shown in Figure 14b for the 54 wt % PS-PI blend. This increasing level of residual deformation, after a deformation at large strains, indicates the presence of a very slowly relaxing structure.

Interestingly, for the blends diluted with resin, the effect of the PS-PI content is qualitatively the same: the blend shows nearly no residual deformation when there is no diblock as shown in Figure 15a and becomes more and more modified by the successive tractions when diblock chains are added (Figure 15b). Finally, the two blends with 60 wt % resin and 42 and 54 wt % PS-PI are the most dissipative when the tests are performed at a crosshead velocity of  $V_t = 50 \text{ mm min}^{-1}$ . This is in full agreement with the results obtained in tensile tests which could not be fitted with the slip-tube model.

It is clear that, at large strains, the parameter controlling residual deformation appears to be the diblock content and not the resin content. Indeed, the blends without diblock are quite elastic regardless of the amount of resin. However, the presence of resin in the blend enhances the instantaneous dissipative losses for all blends.

This result is very interesting and deserves to be discussed further. As can be seen from Figure 1, the tackifying resin is a rather bulky and stiff molecule. Because of its high  $T_g$ , it clearly influences the mean

molecular friction in the rubbery domains, and this is reflected in the increased dissipation observed at small strains (Figure 3) relative to the blends without resin. However, this type of dissipation does not involve any change in structure of the adhesive blend and does not leave much residual deformation once the force returns to zero after a tensile test.

On the other hand, the diblock chains which are entangled within the rubbery domains become disentangled by the large deformation and require an exponentially long time to return to their original conformation. As a result, an increasing amount of residual strain is observed with increasing diblock content.

Even though the tests were performed to detect a Mullins effect, no real Mullins effect was identified in our materials. Indeed, the dissipation of energy we measured does not seem to be due to the systematic breakage of an organized structure but more to a progressive and slow disentanglement of the diblock chains, causing viscoelastic dissipation at the macromolecular scale. It is interesting to note that the presence of resin, despite causing an important increase in the monomer friction coefficient at room temperature, did not affect greatly the measured residual strain while the presence of diblocks had a significant effect.

## 7. Conclusions

We have performed a detailed investigation of the mechanical properties of blends of diblock and triblock copolymers in the large strain regime. We focused our investigation on block copolymers with a low volume fraction of PS varying from 6 to 15%, typical of those used in hot melt and pressure-sensitive adhesives applications.

These materials behave very similarly to cross-linked rubbers with however some significant differences. First of all they all exhibit a pronounced strain softening followed by a strain hardening in uniaxial extension. This behavior can be analyzed with rubber elasticity models and is due to an entangled but weakly cross-linked structure. The diblock/triblock ratio controls the entanglement/cross-link ratio and has a spectacular effect on the large strain properties, in particular the addition of a significant fraction of diblock cause a very pronounced strain softening, which in nominal strain terms can causes a decrease in stress with increasing extension.

The behavior of these physically cross-linked polymeric materials can be modeled with some success with a molecularly based model. However, the PS nodules are not cross-link points, and at high diblock content and high resin content the fit of the model becomes poor mainly because of the increasingly viscoelastic behavior of the material. Furthermore, if the density of triblock bridging chains is taken as the sole source of physical cross-links, the molecular model significantly underestimates the effect of the diblock on the large strain properties.

The blends display a marked nonlinear viscoelastic behavior and are much more dissipative at low strains than at high strains. This suggests that free diblock chains dangling from PS domains may have very long relaxation times, which dominate the viscoelastic behavior at low strains, while at high strains the behavior is dominated by the bridging chains provided by the triblocks.

These studies suggest that it is generally possible to tune both nonlinear elastic properties and linear viscoelastic properties of block copolymer based materials by controlling the ratio of bridging chains vs dangling chains in the blend. In that case more complicated architectures such as radial copolymers and grafted copolymers could provide a simple way to control these two parameters or to reach higher levels of densities of bridging chains without increasing the viscosity too much above the order-disorder transition.

**Acknowledgment.** We gratefully acknowledge the financial support of the European Commission under the GROWTH programme of the 5<sup>th</sup> framework (Collaborative project No. G5RD-CT2000-00202 DEFSAM). We are also indebted to Ken Lewtas, Jacques Lechat, and Galina Ourieva from ExxonMobil Chemical Europe for supplying the raw materials and to all the participants in the DEFSAM project for many helpful discussions.

## References and Notes

- (1) Creton, C.; Kramer, E. J.; Brown, H. R.; Hui, C. Y. *Adv. Polym. Sci.* **2002**, *156*, 53–136.
- (2) Ewins, E. E.; St. Clair, D. J.; Erickson, J. R.; Korcz, W. H. In *Handbook of Pressure-Sensitive-Adhesive technology*, 2nd ed.; Satas, D., Ed.; Van Nostrand Reinhold: New York, 1989; Vol. 1, pp 317–373.
- (3) Brown, K.; Hooker, J. C.; Creton, C. *Macromol. Mater. Eng.* **2002**, *287*, 163–179.
- (4) Nakajima, N.; Babrowicz, R.; Harrell, E. R. *J. Polym. Sci., Polym. Phys. Ed.* **1992**, *44*, 1437–1456.
- (5) Kraus, G.; Jones, F. B.; Marrs, O. L.; Rollmann, K. W. *J. Adhes.* **1977**, *8*, 235–258.
- (6) Guth, E. *J. Appl. Phys.* **1945**, *16*, 20–25.
- (7) de Gennes, P. G. *Scaling Concepts in Polymer Physics*, 2nd ed.; Cornell University Press: Ithaca, NY, 1979.
- (8) Daoulas, K.; Theodorou, D. N.; Roos, A.; Creton, C. *Macromolecules* **2004**, *37*, 5093–5109.
- (9) Gibert, F. X.; Marin, G.; Derail, C.; Allal, A.; Lechat, J. *J. Adhes.* **2003**, *79*, 825–852.
- (10) Christensen, S. F.; Everland, H.; Hassager, O.; Almdal, K. *Int. J. Adhes. Adhes.* **1998**, *18*, 131–137.
- (11) Shull, K. R.; Creton, C. *J. Polym. Sci., Part B: Polym. Phys.* **2004**, *42*, 4023–4043.
- (12) Derail, C.; Allal, A.; Marin, G.; Tordjeman, P. *J. Adhes.* **1997**, *61*, 123–157.
- (13) Verdier, C.; Piau, J. M.; Benyahia, L. *J. Adhes.* **1998**, *68*, 93–116.
- (14) Mullins, L. *Rubber Chem. Technol.* **1957**, *30*, 555–571.
- (15) Bueche, F. *J. Appl. Polym. Sci.* **1960**, *4*, 107–114.
- (16) Kaelble, D.; Cirlin, E. *J. Polym. Sci., Polym. Symp.* **1973**, *43*, 131–148.
- (17) Chen, Y. D. M.; Cohen, R. E. *J. Appl. Polym. Sci.* **1977**, *21*, 629–643.
- (18) Holden, G.; Bishop, E. T.; Legge, N. R. *J. Polym. Sci., Part C: Polym. Symp.* **1969**, *26*, 37–57.
- (19) Sato, T.; Watanabe, H.; Osaki, K. *Macromolecules* **1996**, *29*, 6231–6239.
- (20) Hotta, A.; Clarke, S. M.; Terentjev, E. M. *Macromolecules* **2002**, *35*, 271–277.
- (21) Prasman, E.; Thomas, E. L. *J. Polym. Sci., Part B: Polym. Phys.* **1998**, *36*, 1625–1636.
- (22) Gent, A. N. In *Engineering with Rubber*; Gent, A. N., Ed.; Hanser: Munich, 1992; pp 33–66.
- (23) Rubinstein, M.; Panyukov, S. *Macromolecules* **2002**, *35*, 6670–6886.
- (24) Mooney, M. *J. Appl. Phys.* **1940**, *11*, 582.
- (25) Rivlin, R. S. *Philos. Trans. R. Soc. London, Ser. A* **1948**, *241*, 379–397.
- (26) Creton, C. *MRS Bull.* **2003**, *28*, 434–439.
- (27) Holt, W. L. *Rubber Chem. Technol.* **1932**, *5*, 79–89.
- (28) Frischknecht, A. L.; Milner, S. T.; Pryke, A.; Young, R. N.; Hawkins, R.; McLeish, T. C. B. *Macromolecules* **2002**, *35*, 4801–4820.
- (29) Ferry, J. D. *Viscoelastic Properties of Polymers*, 3rd ed.; Wiley: New York, 1980; Vol. 1.

- (30) Fetters, L. J.; Lohse, D. J.; Colby, R. H. In *Physical Properties of Polymers Handbook*; Mark, J. E., Ed.; American Institute of Physics: New York, 1996; pp 335–340.
- (31) Roos, A. Université Paris VI, Paris, 2004.
- (32) Washiyama, J.; Kramer, E. J.; Hui, C. Y. *Macromolecules* **1993**, *26*, 2928–2934.
- (33) Note that this corresponds to a frequency of  $\sim 17$  Hz, i.e., a pulsation of  $\sim 105$  rad s<sup>-1</sup>. Thus, with the linearity test done previously we are sure to be in the linear regime.

MA050322T